Kinetics, isotherm, and thermodynamics of oil spill removal from seawater onto mango leaves

Ahmed Abutaleb

Chemical Engineering Department, College of Engineering, Jazan University, Jazan, Saudi Arabia, Tel. +966 59 799 7716, email: Azabutaleb@Jazanu.edu.sa

ABSTRACT

In this study, mango leaves, an agricultural biomass waste, were assessed as adsorbent biomass for oil removal from seawater by adsorption. Mango leaves were investigated by wettability and Fourier-transform infrared spectroscopy analysis. In the exothermic system, the maximum oil sorption capacity of biomass reached (6.66 g/g) at 3 min and 0.15 g dose of biomass. The oil sorption outcomes were studied by kinetic and isotherm studies, and the outcomes showed that the oil uptake was fitted with the pseudo-second-order kinetic (R^2 = 0.9921; χ^2 = 0.0347) and Redlich–Peterson (R^2 = 0.9982; χ^2 = 0.0134) models. Also, the economic recycling of biomass was evaluated. The effective oil-adsorbing ability of mango leaves made them good adsorbent material for oil spill removal and for being used in an oil/water purification system.

Keywords: Oil spill; Mango leaves; Isotherm; Kinetics; Thermodynamics

1. Introduction

Industrial development and competition have significantly increased the energy demand. Oil is one of the main sources of energy. Numerous industries and other sectors rely heavily on it. Increasing demand for oil and its transportation across seas and oceans has exposed surface waters to being polluted by oil and its derivatives [1]. Leaked oil affects oil factories given the danger of fires, in addition to the threat it poses to desalination plants, in the event of drinking water getting contaminated by oil [2]. Oil pollution of the seas negatively affects such economic activities as fishing, tourism, and gas exploration, among others [3]. Oil transportation, accidents, wars, and exploration operations are among the factors that cause oil pollution [4]. Much research is underway to find modern, effective, and quick ways to alleviate the oil spillage from water to remedy the environmental impacts of the leakage/spillage [5]. Time is among the most key factors when it comes to removing oil pollution from these waters to prevent it from

reaching the shores, as this is important if economic loss from the spillage is to be kept low [6]. The oil chemical composition contains four main compounds saturated, aromatics, resins and asphaltenes. Spilled oil can interact with suspended particles (mineral or organic) in aquatic environments and form aggregates, including oil-mineral-aggregates which settle in the seedbed [7]. Oil pollution can be bio-controlled by bacteria. Some scientists have reported that some microorganisms can analyze petroleum materials and convert oil slicks into very fine drops in water [8]. Another remedial measure is the use of devices that skim the thick oil layer floating above the surface of the water, and the skimmed oil is then collected and withdrawn using pumps [9]. Oil adsorption generally occurs in three steps: the diffusion of oil molecules into the sorbent surface, their entrapment in the sorbent structure by capillary action, and the agglomeration of oil droplets in the porous and rough structure of the sorbent [10]. Sorption is carried out in two mechanisms, absorption and adsorption. Sorbents allow oil to penetrate pore spaces of material, while sorbents attract

oil to their surfaces but do not allow it to penetrate into the material [11]. Sorption is a favorable process and cost-effective technique to decrease the environmental problems of the oil spills [12]. Oil adsorption generally occurs in three stages: the diffusion of oil particles into the sorbent surface, their entrapment in the sorbent structure by capillary action, and the agglomeration of oil droplets in the porous and coarse structure of the sorbent [13]. The process of adsorption is also used to remove oil pollution, using adsorbent materials such as flax fiber [9], green materials [14], graphene oxide/β-cyclodextrin [15], banana peels [8], graphene/polyethylene nanocomposite [16], sugarcane solid residue [17], cotton fibers [18], orange peel waste [19], wheat straw [20], and carbonized rice husk [21]. In the research work presented here, the potential of mango leaves to adsorb oil from seawater was studied. The controlling factors in the sorption process, such as the sorption time, oil ratio, adsorbent dose, and temperature were optimized. Also, sorption models and thermodynamics of the sorption process were studied. The recycling potential of mango biomass after using it for oil spill removal from seawater and the economic feasibility, on the whole, of using mango biomass for this purpose were evaluated.

2. Materials and methods

2.1. Materials

Mango leaves were collected from the mango farms. Used oil (viscosity: 58. 94 mm²/s, water content: 0.02%, density: 706 kg/m³) obtained from car maintenance plants. Along with these, seawater (3.5% salinity) was used in this research work.

2.2. Biomass preparation

200g of mango leaves were washed and dried at 105°C. The dried mass was cut into <0.5 cm flakes before being used in the sorption processes. In addition, the biomass was characterized by Fourier-transform infrared spectroscopy (FTIR) and contact angle analysis.

2.3. Methods

The oil ratio (0.3–1.5 g), of used oil was mixed with an adsorbent dose range (0.05–0.45 g) of mango leaves on 1 L seawater in a glass vessel at operating sorption conditions of 28°C. Sorption time variety (0.5–4.5 min), oil ratio (0.3–1.5 g), and temperature range (28°C–50°C) were studied. At equilibrium, the oil-loaded biomass was separated, drained for 3 min, and dried at 105°C for 12 h to remove sorbed water and then re-weighted (Electronic Analytical Balance, Model: ALE-223). The experiment test was carried out three times and the results are taken as the average for the accuracy of obtaining the results.

The water (W_C) (g) and oil (O_S) (g) sorbed were determined using the following equations:

$$W_C\left(g\right) = W_{(W+O)} - W_{D(O)} \tag{1}$$

$$O_S\left(g\right) = W_{D(O)} - W_F \tag{2}$$

where $W_{(W+O)}$, $W_{D(O)}$ and W_F are the weights of biomass with oil and water, dried wet (oil) biomass and primary weight of biomass, respectively.

Also, the percent of oil sorption (P_{os}%) was determined by Eq. (3):

$$P_{OS}\% = \frac{\left(W_{D(O)} - W_F\right)}{W_F} \times 100 \tag{3}$$

where $W_{(W+O)}$, $W_{D(O)}$ and W_F are the weights of biomass with oil and water, dried wet (oil) biomass, and primary weight of biomass, respectively.

Also, the percentage of oil sorption (P_{os}%) was determined by the following equations:

At equilibrium, the sorption capacity of biomass q_e (g/g) can be determined by using the following equation:

$$q_e = \frac{O_S}{W_F} \tag{4}$$

3. Results and discussion

3.1. Characterization

3.1.1. FTIR analysis

The FTIR pattern (Thermo Fisher Scientific, USA) of mango leaves shows that the leaves include many functional groups that characterize the mango leaves. In Fig. 1, it was found that the hydroxyl group is present at the band at 3,475 cm⁻¹ that occurs in cellulose [22]. While the C–H group is located at 2,942 cm⁻¹ [23]. Also, the C=O group appeared at 1,730 and 1,535 cm⁻¹ [9]. The –C–H group and CH₂ vibrations looked at band 1,377 cm⁻¹. The bands at 1,160–1,125 cm⁻¹ refer to the asymmetric C–O–C group, whereas the band at 600 cm⁻¹ denotes to C–O group of ether [24]. Functional groups present in the mango leaves can be characterized as hydrophobic or hydrophilic nature based on their polarity features. FTIR investigation showed that mango leaves have hydrophilic in nature in the hydroxyl (OH), carbonyl (C=O) and carboxyl (COOH)) groups and hydrophobic nature in the methyl (C–H), ester (R–COO–R) and ether (C–O–C) groups [25,26]. These results increase the oil sorption interaction with mango leaves.

3.1.2. Wettability investigation

Fig. 2 displays the contact angle analysis (Krüess Processor Tensiometer K100) of oil and seawater on the biomass surface. Fig. 2a shows a high contact angle (115.33°) of biomass with water, whereas the contact angle of 23.19° appeared in the biomass surface with oil (Fig. 2b), indicating the lipophilic and hydrophobic properties of mango leaves structure, which increase the oil uptake than water from the sorption system.

3.2. Sorption dynamics

3.2.1. Sorption time effect

The sorption time was optimized in the variety (0.5–4.5 min) by contact of 0.1 g of biomass on 0.5 g oil in 1 L
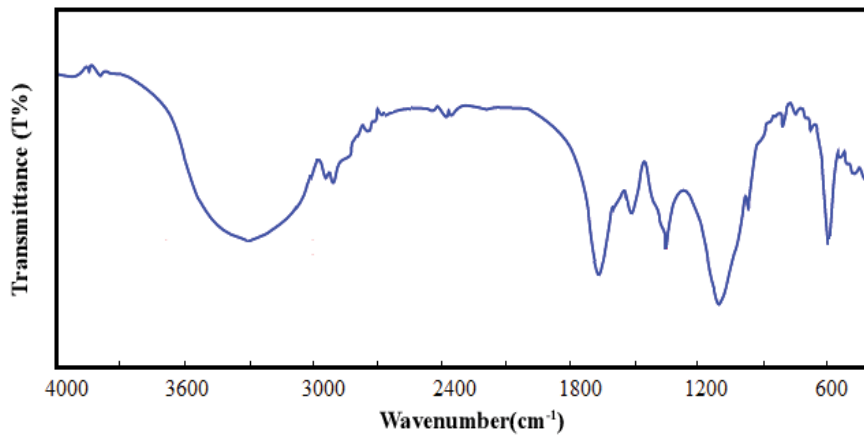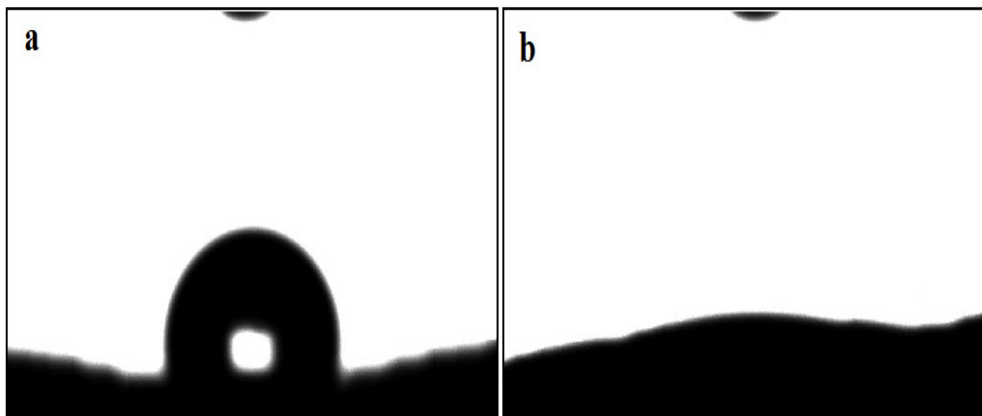
Fig. 1. FTIR analysis of mango leaves.

Fig. 2. Contact analysis of mango leaves with (a) water and (b) used oil.

seawater in a glass vessel at 28°C. The sorption data displays that the equilibrium oil removal percentage (P_{os}% = 80.12%) and oil sorption capacity (4.012 g/g) were reached at the end of 3 min. The results (Fig. 3a) show that the fast oil uptake during the preliminary period (0.5–3 min) was because of the excellent oleophilic interaction and the sorption capillary force of biomass increased the oil removal percentage, which [9]. In addition, the initial high oil sorption capacity and P_{os}% of oil can be attributed to the presence of unfilled active sites on the surface of biomass and also due to the reducing strong attractive forces between the oil molecules and the biomass as the contact sorption time increased [27]. No significant increase in the oil removal percentage was achieved after 3 min because of the richness of the oil uptake sites of leaves [28].

3.2.2. Effect of biomass dose

The range (0.05–0.45 g) of biomass dose was used to determine the optimum dose on the oil sorption system (0.5 g oil/1 L seawater) under operating conditions (28°C and 3 min). Fig. 3b depicts that the increase in the biomass dose from 0.05 to 0.15 g increases the oil removal percent until reached 99.99% with 0.15 g dose. Whereas no noticeable change is observed with, the increased in the biomass

and this can be considered as an economic loss in the use of the adsorbent material, owing to the sorption of all oils in the oil sorption system [9,29]. In addition, an increase in the biomass dose reduces the sorption capacity of biomass. Meanwhile, the reduction in the oil sorption capacity was principally due to the higher unsaturated sorption sites available during the sorption process [16,21].

3.2.3. Effect of oil dose

The oil feed range (0.3–1.5 g) in the sorption system was kept this way to determine the maximum oil sorption capability of biomass at optimum operating conditions (28°C, 3 min, and 0.15 g b dose). Fig. 4a depicts that the oil sorption uptake of biomass improved from 1.8 to 6.66 g/g with an increase in the inlet oil feed from 0.3 to 1 g due to the availability of active sites on the surfaces of the biomass. Conversely, when the initial crude oil concentration was increased, the number of active adsorption sites was not enough to accommodate crude oil molecules, thus leading to a lower adsorption capacity [30]. However, the oil removal percent dropped from 99.98% to 66.60% with an increase in the inlet oil feed from 0.3 to 1.5 g/L, owing to the richness of uptake sites in the biomass [31].

3.2.4. Temperature effect

Heat is an imperative element in the cleaning of oil spillage because of its effect on the viscosity of oil and the adsorption capillary force of the biomass surface [21]. Fig. 4b shows that the uptake of biomass declines from 6.66 to 2.90 g/g with an increase in the temperature from 28°C to 50°C. The reduction in the capacity of biomass is because of the increase in oil solubility, caused by decreasing its viscosity as the temperature increased, which led to increases in the reduction mass of the oil adsorbed from biomass during the draining stage [19]. In addition, an increase in both

% removal of crude oil and adsorption capacity at lower temperatures was possibly due to an increase in kinetic forces [32].

3.3. Sorption kinetics

Non-linear kinetic models were employed to study the sorption outcomes of oil spills onto mango leaves. The kinetic fitting with experimental outcomes was investigated by the values of correlation coefficient (R^2) and chi-square analysis (χ^2) [9].
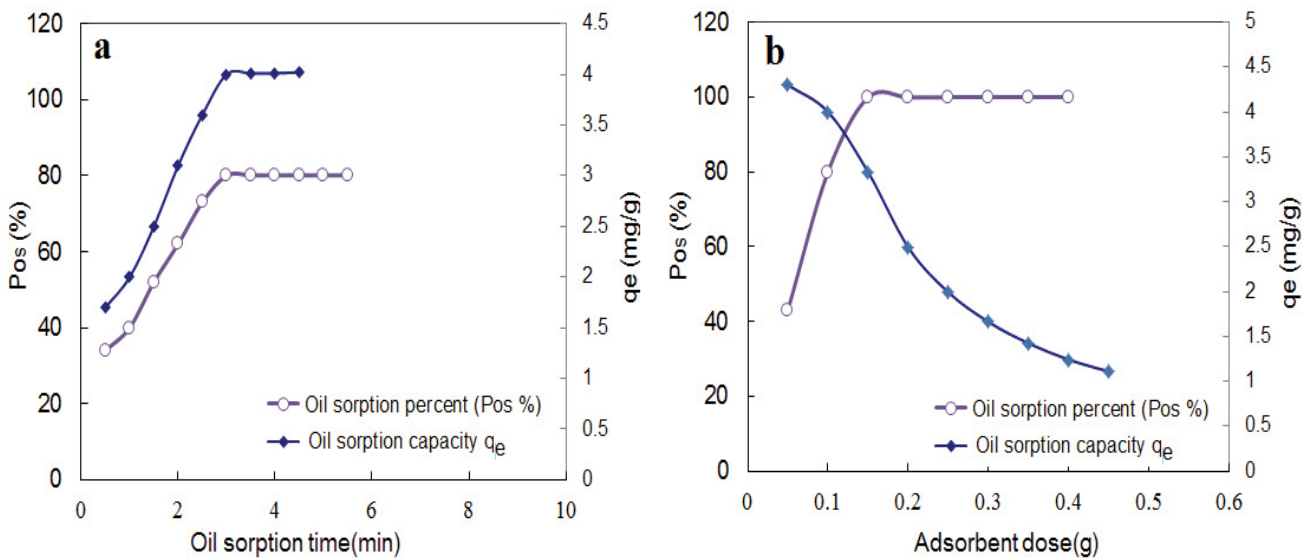

Fig. 3. Sorption time (0.5 g oil/1 L seawater; 28°C; 0.1 g of biomass) (a) adsorbent dose (0.5 g oil/1 L seawater; 28°C; 3 min) and (b) plots of oil sorption onto mango leaves from oil/seawater sorption.
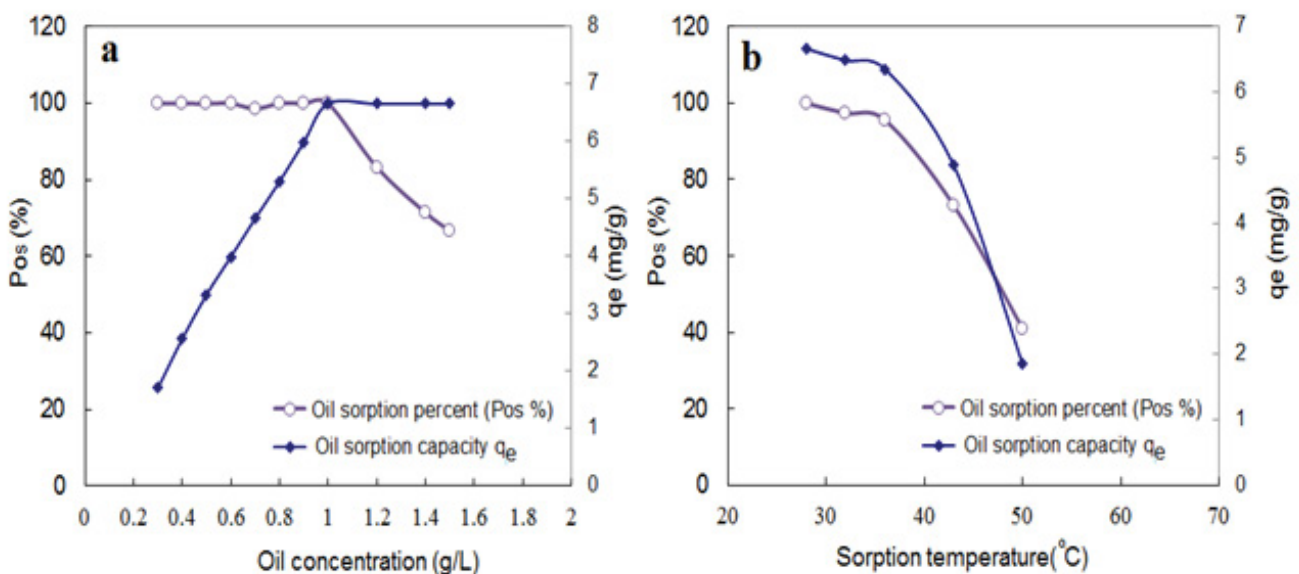

Fig. 4. Sorption dynamics: oil concentration (28°C; 3 min; 0.15 g biomass dose) (a) sorption temperature (1.0 g oil dose; 3 min; 0.15 g biomass dose) and (b) of oil sorption onto mango leaves from oil/seawater sorption.

$$R^2 = \frac{\sum_{i=1}^{n}\left(q_{e \text{ experimental}} - q_{e \text{ calculated}}\right)^2}{\sum_{i=1}^{n}\left(q_{e \text{ experimental}} - q_{e \text{ calculated}}\right)^2 + \sum_{i=1}^{n}\left(q_{e \text{ experimental}} - q_{e \text{ calculated}}\right)^2} \quad (5)$$

$$\chi^2 = \sum_{i=1}^{n} \frac{\sum_{i=1}^{n}\left(q_{e \text{ experimental}} - q_{e \text{ calculated}}\right)^2}{q_{e \text{ calculated}}} \quad (6)$$

Pseudo-first-order model [33]:

$$q_t = q_e\left(1 - e^{-k_1 t}\right) \quad (7)$$

Pseudo-second-order model [27]:

$$q_t = \frac{K_2 q_e^2 t}{\left(1 + K_2 q_e t\right)} \quad (8)$$

The Elovich kinetic model [9]:

$$\frac{dq_t}{dt} = \alpha \exp\left(-\beta dt\right) \quad (9)$$

where q_t (g/g): the uptake at time t; q_e (g/g): the uptake at equilibrium; K_1 (L/min): pseudo-first-order constant; K_2 (g/mg·min): pseudo-second-order constant; α and β: constants Elovich model.

Table 1 displays the results of sorption kinetics, which indicate that the theoretical q_e (6.4321 g/g) of the pseudo-second-order model is a covenant with sorption q_e (6.66 g/g). It also indicates that the greater R^2 (0.9921) and lesser χ^2 (0.0347) of the pseudo-second-order model rather than the pseudo-first-order model and Elovich kinetic models demonstrate the greatest fit of experimental results with the pseudo-second-order model as can be seen in Fig. 5a, which illustrates the physiochemical sorption of oil uptake onto mango leaves. This also explained that the rate of oil uptake was controlled by chemisorption, which involved co-valent forces concluded the sharing of

Table 1
Results of non-linear sorption kinetics under conditions (0.5 g oil/1 L seawater; 28°C and 0.1 g of biomass)

Kinetic models	Parameter	Values
Pseudo-first-order	q_e (g/g)	5.1240
	K_1 (L/min)	2.8741
	R^2	0.9123
	χ^2	1.1321
Pseudo-second-order	q_e (g/g)	6.4321
	K_2 (g/mg·min)	0.2741
	R^2	0.9921
	χ^2	0.0347
Elovich	β	4.7710
	α	1.0321
	R^2	0.8821
	χ^2	1.3541

electrons between the biomass and oil molecules. In addition, the rates of surface reaction and transference of oil from seawater to biomass phase were faster due to the high hydrophobic nature of the biomass [18,33].

3.4. Sorption isotherm modeling

To describe the stability of oil uptake onto mango leaves, the sorption outcomes were modeled by non-linear sorption isotherms. The isotherm models are defined by the following equations:

Langmuir isotherm [9,28]:

$$q_e = \frac{Q_L K_L C_e}{1 + K_L C_e} \quad (10)$$

Freundlich isotherm [21]:

$$q_e = K_F C_e^{1/n} \quad (11)$$

Redlich–Peterson isotherm [19]:

$$q_e = \frac{K_{RP} C_e}{\left(1 + A C_e^{\beta}\right)} \quad (12)$$

where C_e (g/g): the oil concentration at equilibrium; K_L (L/min) and Q_L (g/g): Langmuir constants; K_F (g/mg·min) and n: Freundlich constants; K_{RP} (L/g), A (L/g)$^{\beta}$ and β: constants of Redlich–Peterson model.

Fig. 5b depicts the scheme of sorption isotherms at 28°. Table 2 shows that the Redlich–Peterson isotherm gives more accurate and good fitting (R^2 = 0.9982; χ^2 = 0.0134) for oil uptake onto mango leaves when compared with the results of the Langmuir, Freundlich models, clarifying that the mechanism of oil sorption onto mango leaves is a mix of multi and monolayer sorption.

3.5. Thermodynamic studies

The thermodynamics of the sorption process was studied to investigate the oil uptake onto mango biomass. The thermodynamic parameters (enthalpy ($\Delta H°$), Free energy ($\Delta G°$), and entropy ($\Delta S°$)) were determined based on the results of the following equations [29]:

$$\Delta G = -RT \log K_c \quad (13)$$

$$\Delta G = \Delta H - T\Delta S \quad (14)$$

$$\ln K_c = \frac{\Delta S}{R} - \frac{\Delta H}{RT} \quad (15)$$

$$K_c = \frac{q_e}{C_e} \quad (16)$$

where C_e is the oil concentration (g/L) at equilibrium, R is the gas constant (8.314 J/mol K), and T is the temperature (K). Fig. 6a shows the Van't Hoff plot of oil uptake onto mango biomass. The results (Table 3) indicate that negative free
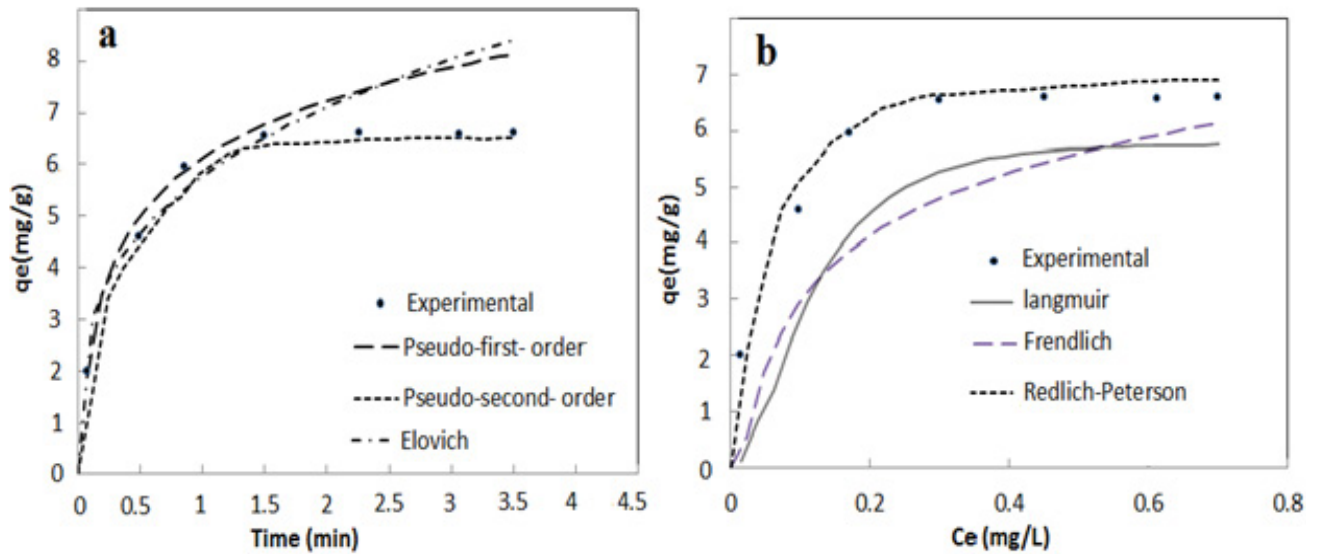
Fig. 5. Kinetic (0.5 g oil/1 L seawater; 28°C; 0.1 g of biomass) (a) and isotherm (28°C; 3 min; 0.15 g biomass dose) and (b) models of used oil uptake onto mango leaves.

Table 2
Results of non-linear sorption isotherm studies under conditions (28°C; 3 min; 0.15 g biomass dose)

Isotherm model	Parameter	Values
Langmuir isotherm	Q_L (g·oil/g·biomass)	5.1511
	K_L (L/g)	3.2140
	R^2	0.9882
	χ^2	0.1134
Freundlich isotherm	K_F (g$^{(1-1/n)}$/L$^{1/n}$·g)	5.3214
	n	5.2451
	R^2	0.9354
	χ^2	1.2741
Redlich–Peterson isotherm	K_{RP} (L/g)	5.4880
	P (L/g)$^\beta$	12.213
	β	5.5471
	R^2	0.9982
	χ^2	0.0134

Table 3
Thermodynamic sorption studies under operating conditions (1.0 g oil dose; 3 min; 0.15 g biomass dose)

T (K)	ΔG (kJ/mol)	ΔH (kJ/mol)	ΔS (kJ/mol·K)
301	−17.539		
309	−13.131		
316	−9.274	−183.39	−0.551
323	−5.417		

$$D_P\left(\%\right) = \left[\frac{W_{D(O)} - W_{sq}}{W_{D(O)} - W_F} \right] \times 100 \tag{17}$$

where W_{sq} refers to the contents (g) of oil after the pressing technique. The results seen in Fig. 6b indicate that the reusability of biomass reduced with increasing sorption-squeezing cycles, owing to the decrease in the oil uptake capacity of mango biomass. The economic effectiveness of biomass dropped under 50% after five adsorption–desorption cycles, indicating that the use of mango leaves for oil removal from the oil/seawater system is economically feasible. The depleted biological material after reuse is considered solid waste that is considered to be a pollutant in the environment, but this problem can be solved and environmental pollution was prevented by using this material to generate energy in many processes such as those of steam production by boilers and running rotary kilns in the cement industry. Table 4 presents a comparison of the economic use of mango leaves with other adsorbents. The results suggest that compared to other sorbents, mango leaves are more effective as an oil sorbent in the process of oil removal from the oil/seawater system.

energy decreases with elevated temperature, representing the favorability of oil uptake onto biomass. In addition, negative enthalpy shows exothermic oil sorption. Positive entropy denotes the randomness of oil interaction with biomass [27].

3.6. Reusability studies

One of the important factors in selecting the adsorbent material is the ability to reuse it more than once, which increases its economic value vis-à-vis removing oils [9]. The recycling system was implemented by pressing the loaded biomass between a cylindrical pressure system called squeezing rollers. The oil desorption percent (D_P%) was determined by the following equation:
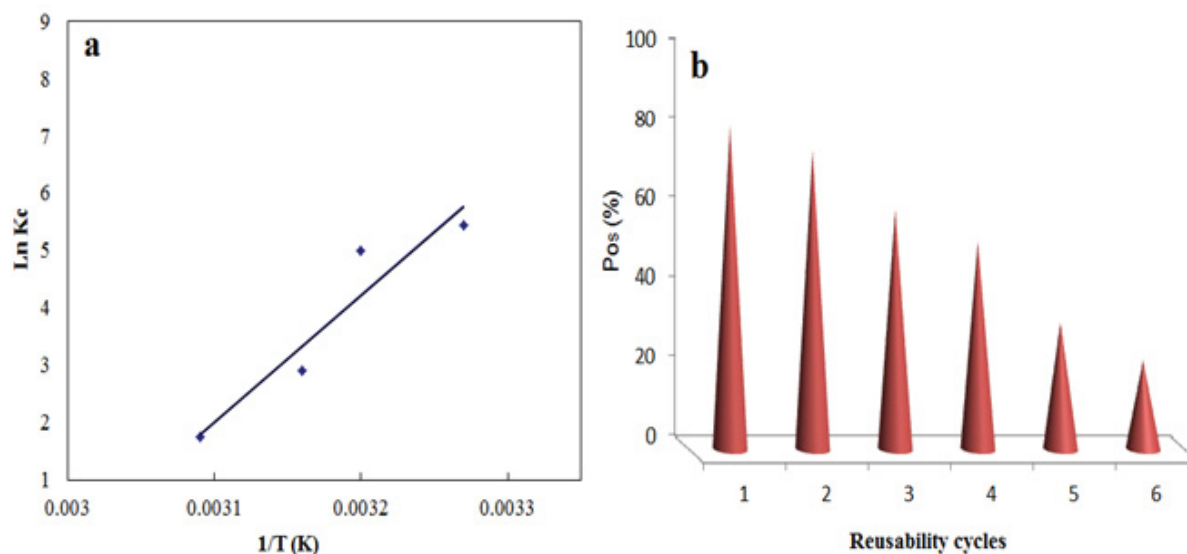
Fig. 6. Van't Hoff plot (1.0 g oil dose; 3 min; 0.15 g biomass dose) (a) and reusability cycles (1.0 g oil dose; 3 min; 0.15 g biomass dose; 28°C) and (b) of oil uptake onto biomass.

Table 4
Evaluation of oil uptake of mango biomass with other biomasses

Sorbent material	Sorption capacity (g/g)	References
Banana peel	6.35	[16]
Bagasse	11.3	[23]
Sawdust	6.4	[24]
Sisal	6.4	[24]
Raw kapok fiber	38.1	[5]
Wheat straw	4.0	[20]
Flax fiber	13.75	[9]
Mango leaves	6.66	Present study

4. Conclusion

Mango leaves displayed good oil adsorbent capacity for removal of oil from the oil/seawater system. The batch sorption indicated that oil uptake depends on the sorption time and biomass dose of mango leaves. The oil sorption capability reached the highest value (6.66 g/g) at 3 min and 0.15 g dose of biomass in an exothermic oil sorption system. The experimental outcomes were also modeled using kinetic and isotherm studies. The pseudo-second-order kinetic and Redlich–Peterson models were found to be fitting the experimental results well. The mechanism of oil uptake of mango leaves was controlled by fiber uptake on the biomass surface and capillary sorption by the biomass cavities. The sorption efficiency of mango leaves reduced to below 50% of their sorption capacity after they was reused for 5 cycles.

References

[1] M. Mojžiš, T. Bubeníková, M. Zachar, D. Kačíková, J. Štefková, Comparison of natural and synthetic sorbents' efficiency at oil spill removal, BioResources, 14 (2019) 8738–8752.

[2] P.K. Andy Hong, T. Xiao, Treatment of oil spill water by ozonation and sand filtration, Chemosphere, 91 (2013) 641–647.

[3] S.E. Allan, B.W. Smith, K.A. Anderson, Impact of the deepwater horizon oil spill on bioavailable polycyclic aromatic hydrocarbons in Gulf of Mexico coastal waters, Environ. Sci. Technol., 46 (2012) 2033–2039.

[4] H. Zhu, S. Qiu, W. Jiang, D. Wu, C. Zhang, Evaluation of electrospun polyvinyl chloride/polystyrene fibers as sorbent materials for oil spill cleanup, Environ. Sci. Technol., 45 (2011) 4527–4531.

[5] J. Wang, Y. Zheng, A. Wang, Superhydrophobic kapok fiber oil-absorbent: preparation and high oil absorbency, Chem. Eng. J., 213 (2012) 1–7.

[6] J.C. Onwuka, E.B. Agbaji, V.O. Ajibola, F.G. Okibe, Treatment of crude oil-contaminated water with chemically modified natural fiber, Appl. Water Sci., 8 (2018) 86, doi: 10.1007/s13201-018-0727-5.

[7] C. Wong, T. McGowan, S.G. Bajwa, D.S. Bajwa, Impact of fiber treatment on the oil absorption characteristics of plant fibers, BioResources, 11 (2016) 6452–6463.

[8] G. Alaa El-Din, A.A. Amer, G. Malsh, M. Hussein, Study on the use of banana peels for oil spill removal, Alexandria Eng. J., 57 (2018) 2061–2068.

[9] M.A. Mahmoud, Oil spill cleanup by raw flax fiber: Modification effect, sorption isotherm, kinetics and thermodynamics, Arabian J. Chem., 13 (2020) 5553–5563.

[10] S. Sabir, Approach of cost-effective adsorbents for oil removal from oily water, Crit. Rev. Environ. Sci. Technol., 45 (2015) 191–194.

[11] M. Zamparas, D. Tzivras, V. Dracopoulos, T. Ioannides, Application of sorbents for oil spill cleanup focusing on natural-based modified materials: a review, Molecules, 25 (2020) 4522–4535.

[12] M.A. Mahmoud, Hydrodynamic separator unit for removal and recovery oil from wastewater, J. Pet. Environ. Biotechnol., 7 (2016) 2–8.

[13] X. Yang, M. Guo, Y. Wu, Q. Wu, R. Zhang, Removal of emulsified oil from water by fruiting bodies of macro-fungus (*Auricularia polytricha*), PLoS One, 9 (2014) 95162, doi: 10.1371/journal.pone.0095162.

[14] T.A. Saleh, Protocols for synthesis of nanomaterials, polymers, and green materials as adsorbents for water treatment technologies, Environ. Technol. Innovation, 24 (2021) 101821, doi: 10.1016/j.eti.2021.101821.

[15] A.Q. Al-Gamal, T.A. Saleh, F.I. Alghunaimi, Nanofiltration membrane with high flux and oil rejection using graphene oxide/β-cyclodextrin for produced water reuse, Mater. Today Commun., 31 (2017) 103438, doi: 10.1016/j.mtcomm.2022.103438.

[16] A.B. Olabintan, E. Ahmed, H. Al Abdulgader, T.A. Saleh, Hydrophobic and oleophilic amine-functionalised graphene/polyethylene nanocomposite for oil–water separation, Environ. Technol. Innovation, 27 (2022) 102391, doi: 10.1016/j.eti.2022.102391.

[17] F.B.P.S. Almeida, L. Meili, J. Soletti, K.P.S.O.R. Esquerre, L.M.O. Ribeiro, C.E. de Farias Silva, Oil produced water treatment using sugarcane solid residue as biosorbent, Rev. Mex. Ing. Chim., 18 (2019) 27–38.

[18] J. Wang, F. Han, B. Liang, G. Geng, Hydrothermal fabrication of robustly superhydrophobic cotton fibers for efficient separation of oil/water mixtures and oil-in-water emulsions, J. Ind. Eng. Chem., 54 (2017) 174–183.

[19] I.A. El Gheriany, F.A. El Saqa, A.A. El Razek Amer, M. Hussein, Oil spill sorption capacity of raw and thermally modified orange peel waste, Alexandria Eng. J., 59 (2020) 925–932.

[20] D. Sidiras, F. Batzias, I. Konstantinou, M. Tsapatsis, Simulation of autohydrolysis effect on adsorptivity of wheat straw in the case of oil spill cleaning, Chem. Eng. Res. Des., 92 (2014) 1781–1791.

[21] D. Angelova, I. Uzunov, S. Uzunova, A. Gigova, L. Minchev, Kinetics of oil and oil products adsorption by carbonized rice husks, Chem. Eng. J., 172 (2011) 306–311.

[22] T.A. Saleh, Isotherm, kinetic, and thermodynamic studies on Hg(II) adsorption from aqueous solution by silica-multiwall carbon nanotubes, Environ. Sci. Pollut. Res., 22 (2015) 16721–16731.

[23] T.A. Saleh, K.G. Vinod, Characterization of the chemical bonding between Al_2O_3 and nanotube in MWCNT/Al_2O_3 nanocomposite, Curr. Nanosci., 8 (2012) 739–743.

[24] T.A. Saleh, The influence of treatment temperature on the acidity of MWCNT oxidized by HNO_3 or a mixture of HNO_3/H_2SO_4, Appl. Surf. Sci., 257 (2011) 7746–7751.

[25] T.A. Saleh, Simultaneous adsorptive desulfurization of diesel fuel over bimetallic nanoparticles loaded on activated carbon, J. Cleaner Prod., 172 (2018) 2123–2132.

[26] T.A. Saleh, Carbon nanotube-incorporated alumina as a support for MoNi catalysts for the efficient hydrodesulfurization of thiophenes, Chem. Eng. J., 404 (2021) 126987, doi: 10.1016/j.cej.2020.126987.

[27] A. Abutaleb, A.M. Tayeb, M.A. Mahmoud, A.M. Daher, O.A. Desoukyc, O.Y. Bakather, R. Farouq, Removal and recovery of U(VI) from aqueous effluents by flax fiber: adsorption, desorption and batch adsorber proposal, J. Adv. Res., 22 (2020) 153–162.

[28] J. Huang, Z. Yan, Adsorption mechanism of oil by resilient graphene aerogels from oil–water emulsion, Langmuir, 34 (2018) 1890–1898.

[29] M.A. Mahmoud, Adsorption of U(VI) ions from aqueous solution using silicon dioxide nano powder, J. Saudi Chem. Soc., 22 (2018) 229–238.

[30] R. Behnood, B. Anvaripour, N. Jaafarzadeh, M. Farasati, Oil spill sorption using raw and acetylated sugarcane bagasse, J. Cent. South Univ., 23 (2016) 1618–1625.

[31] T.R. Annunciado, T.H.D. Sydenstricker, S.C. Amico, Experimental investigation of various vegetable fibers as sorbent materials for oil spills, Mar. Pollut. Bull., 50 (2005) 1340–1346.

[32] M. Husseien, A.A. Amer, A. El-Maghraby, N.A. Taha, Availability of barley straw application on oil spill clean-up, Int. J. Environ. Sci. Technol., 6 (2009) 123–130.

[33] O.Y. Bakather, N. Zouli, A. Abutaleb, M.A. Mahmoud, A. Daher, M. Hassan, M.A. Eldoma, S.O. Alaswed, A.A. Fowad, Uranium(VI) ions uptake from liquid wastes by solanum incanum leaves: biosorption, desorption and recovery, Alexandria Eng. J., l59 (2020) 1495–1504.